Slow slip and frictional transition at low temperature at the Hikurangi subduction zone

ROBERT McCAFFREY*, LAURA M. WALLACE AND JOHN BEAVAN

GNS Science, PO Box 30368, Lower Hutt, New Zealand

*e-mail: r.mccaffrey@gns.cri.nz

Published online: 6 April 2008; doi:10.1038/ngeo178

Shallow portions of faults exhibit brittle, stick–slip behaviour that gives way to more stable sliding with increasing depth, limiting the depths to which earthquake-inducing slip can occur. The increase of temperature with depth is often assumed to transform friction in the fault from velocity-weakening (unstable) to velocity-strengthening (stable), and to change conditions from brittle to ductile[1–5]. A temperature of 350 °C has been suggested to mark the base of the frictionally unstable portion of the fault, which becomes free slipping at depth where temperatures rise above 450 °C (refs 2,4,6). Here, we show that both slow-slip events and the geodetically observed transition from fault locking to free slip at the Hikurangi subduction zone east of the North Island, New Zealand occur at temperatures as low as 100 °C, suggesting that temperature is not a primary control on either slow-slip or fault-locking processes at the Hikurangi margin. Although globally shallow slow-slip events are rare, five out of seven events observed so far at the Hikurangi margin are less than 15 km deep.

The depth range within which the transition from stick–slip to free slip occurs on a fault manifests itself differently in various types of observation. The geodetic transition zone (GTZ) is inferred from surface geodetic data and elastic rheology to be the region where interseismic fault locking decreases from nearly complete to zero. The seismic transition zone (STZ) is where seismicity and slip in large earthquakes die out at depth. It is crucial to understand the relationship between the GTZ and STZ if geodetic data are to help further in our assessment of earthquake hazards.

A relatively new class of phenomena associated with this transition are creep episodes, known as slow-slip events (SSEs); such slip events are not associated with large earthquakes. They have been observed at several subduction zones worldwide—Alaska, Cascadia, Mexico, Costa Rica, Japan and New Zealand[5,7] and on the San Andreas fault[8]. They apparently involve a few to tens of centimetres of slip on the fault over days to weeks to years. The causes of SSEs are unknown, yet most viable explanations require conditions that place them within or near the transition from velocity-weakening to velocity-strengthening behaviour[4,9]. Nearly every subduction SSE observed so far has been within the GTZ; proposed exceptions to this rule are not confirmed[4,5].

The Pacific plate subducts westward beneath New Zealand's eastern North Island at the Hikurangi subduction zone (Fig. 1). Campaign global positioning system (GPS) site velocities show that large portions of the subduction thrust are stuck (locked) during the interseismic period[10]. However, the downdip limit of locking (the GTZ) beneath the southern North Island is far deeper (35–50 km) than beneath the northern and central North Island (10–15 km depth) (Fig. 2a). Extensive testing shows that the along-strike change in depth of locking is not an artefact of upper-plate strain rates resulting from other features, such as the Taupo volcanic zone for example[10]. Reyners[11] infers a similar southward increase in the depth of the STZ on the subduction fault from seismological data.

Continuously operating GPS stations in New Zealand from 2002–2007 have recorded seven SSEs, presumably on the Hikurangi subduction zone interface[12–15]. A 10-day-long, 20–30 mm movement in northeastern North Island was observed at two near-coastal GPS sites in October 2002 (ref. 13) (Gs1 in Fig. 2a). A robust estimate of the source region could not be obtained, but slip certainly occurred offshore where the fault is <15 km deep (Fig. 2a). In the same region, two more events occurred in 2004 and 2006 (Gs2 and Gs3; Fig. 2a) for which better estimates of slip have been obtained owing to extra sites. They were also undoubtedly offshore as demonstrated by displacements being maximum and downward at coastal sites. Two events of 9 and 18 days' durations were observed offshore of Hastings in 2006 at less than 15 km depth[14] (Hs1 and Hs2; Fig. 2a). From early 2004 to mid 2005, a well-recorded, long-duration event occurred beneath Manawatu (central North Island)[15] where the slab interface is 30–50 km deep (Fig. 2a). Another possible deep event, on the basis of one site's record[12], occurred in 2003–2004 at 30–45 km depth below the Kapiti Coast north of Cook Strait. Despite the along-strike variability in the depth of the GTZ, Hikurangi SSEs recorded so far have all occurred at or near it (Fig. 2a).

Temperature on the plate-boundary thrust fault is estimated using simple thermal advection[16]. The lithosphere thrusting beneath the overriding plate can either cool or warm the fault zone depending on how fast subduction occurs and on its thermal structure. Such a fault temperature estimate requires knowledge of the age of the subducting plate (determining its thermal structure), the convergence rate normal to the subduction zone and the dip angle (see the Methods section).

The Hikurangi Plateau crust subducting at the Hikurangi margin is Early Cretaceous age thickened oceanic basalt (∼17 km thick)[17]. Although radiogenic heat production in the crust can increase the heat flow, there is no reason to suspect that heat production is any higher in the Hikurangi Plateau crust than in normal oceanic lithosphere, which is negligible.

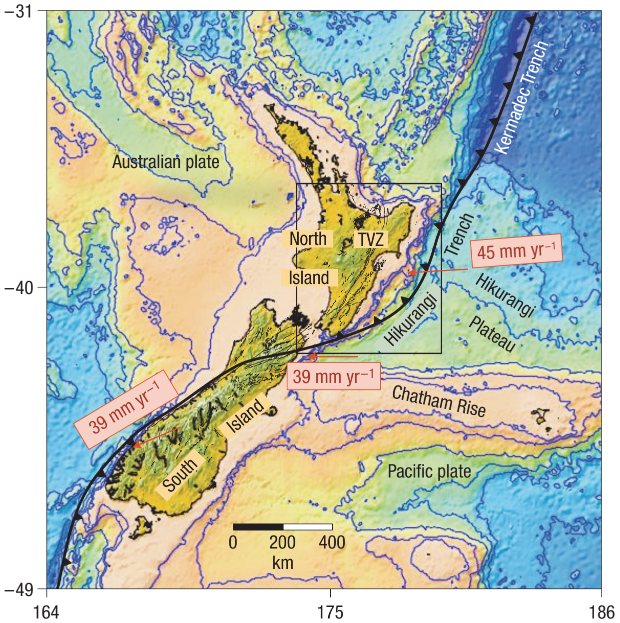

Figure 1 Tectonic and physiographic map of the New Zealand region. Arrows show Pacific plate motion relative to Australia[30]. TVZ: Taupo volcanic zone. Rectangle encloses area of Fig. 2.

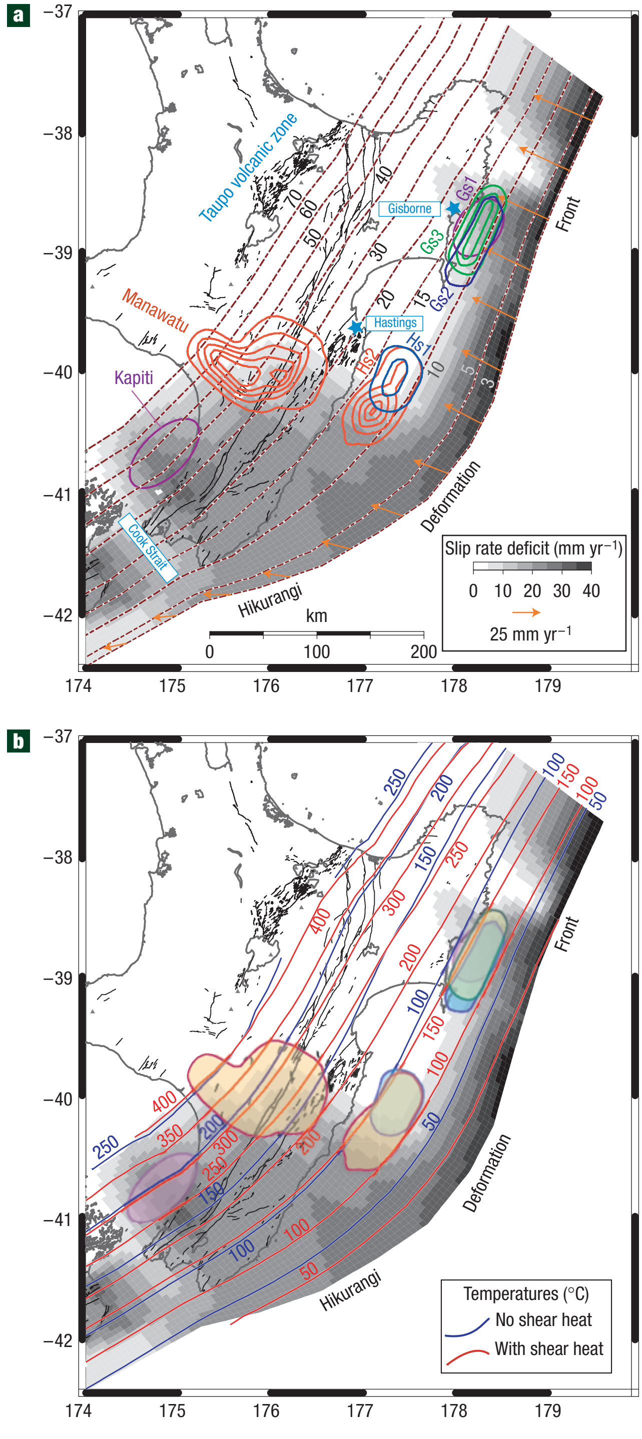

Figure 2 Depth contours, locking distribution, temperatures and slow-slip regions. a, Slab contours[18] (in kilometres below sea level, dashed brown lines) and geodetic locking (slip rate deficit) distribution as greyscale shading[10]. Convergence vectors (orange) are for the Pacific relative to forearc blocks[10]. Coloured contours (50 mm intervals) show SSEs from inversions of geodetic displacements[12–15] (general locations given for poorly constrained Kapiti[12] and Gisborne Gs1[13] events). Hs and Gs refer to numbered SSEs. **b**, Calculated temperature contours (blue for no shear heating; red for shear heating using 20 MPa stress at all depths).

We use an age of 80 Myr for the incoming lithosphere along the length of the subduction zone. At about 80 Myr, the oceanic lithosphere's thermal structure reaches steady state and we expect that the thermal structure within the forearc wedge has reached steady state as well. To estimate convergence at the Hikurangi Trench (Fig. 2a), we use the angular velocities of forearc blocks relative to the Pacific plate based on campaign GPS velocities[10]. The subduction interface (Fig. 2a) from which depths and dip angles are derived is constrained by seismicity[18].

Estimated contours of fault temperature largely follow fault depth contours but deviate along strike owing to changes in dip angle and subduction rate (Fig. 2b; blue contours). By our estimate, the temperature where SSEs occur at the GTZ in the north (near 10–15 km depth) is ~100 °C and in the south it is ~250 °C at 40–60 km depth.

Observed sea-floor heat flow[19–21] varies little along strike within the forearc (Fig. 3) suggesting that subsurface temperature does not vary greatly either. Comparing the heat flow derived from these temperatures with observed surface heat-flow values shows that our initial predictions are lower (blue curves in Fig. 3a and blue circles in Fig. 3b). Next, we explore possible sources of the missing heat flow and whether such sources can preferentially heat the northern part of the fault enough to put the entire transition zone there near 350 °C (see the Methods section).

Forearc thermal conductivity would have to decrease substantially from south to north to allow a ~250 °C increase in fault temperature in the north, but this would also change the heat flow significantly. Moreover, conductivity measurements in wells suggest an increase towards the north[21] that results in northward lowering of temperatures (see the Methods section). The volumetric heat production required to raise the temperature at 20 km depth by 250 °C in the north relative to the south is about 8 μW m^{-3}—this is not only much higher than values observed in forearcs elsewhere[22], it would also increase heat flow in the north by ~30 mW m^{-2}, which is not observed. Sediments blanketing the incoming plate thicken to the south[23] and if anything would contribute to a warmer subduction fault in the south.

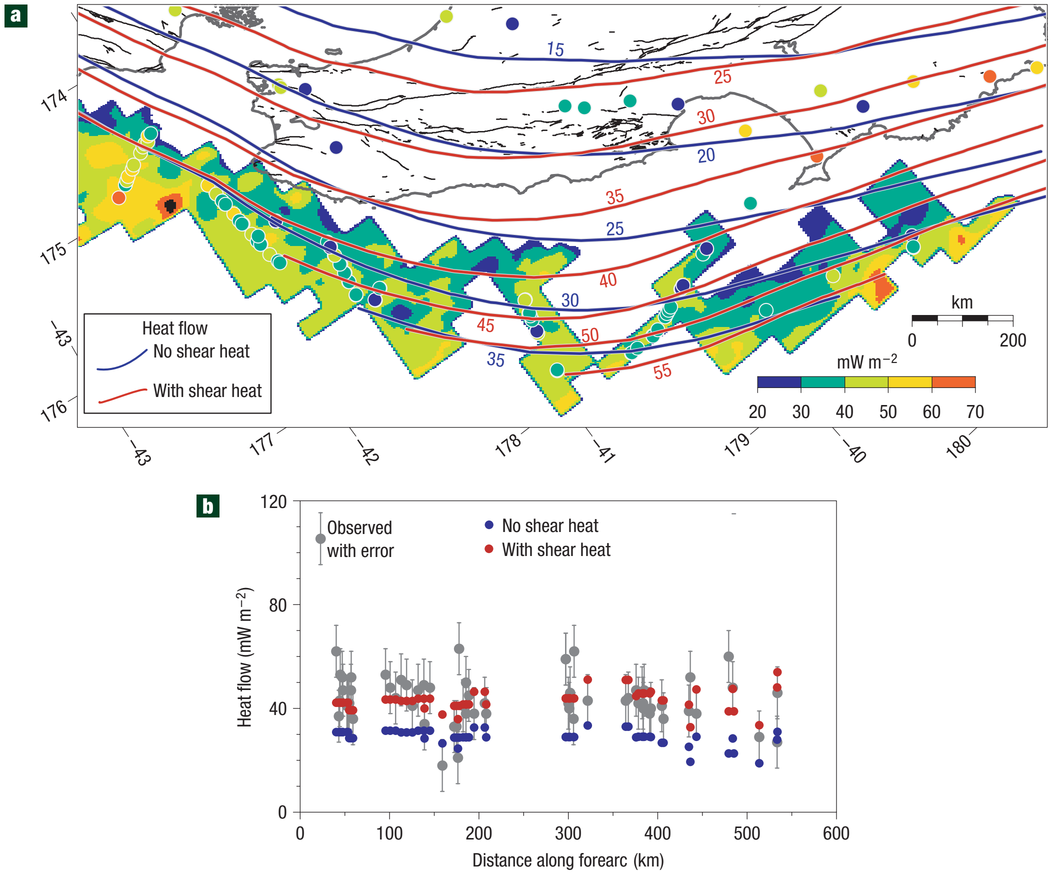

Figure 3 Comparisons of estimated and observed heat-flow values from the Hikurangi margin. a, Circles are from Townend[19] and global heat flow database[21]. Grid is from Henrys *et al.*[20]. Blue curves show estimated heat flow with no shear heating included; red curves show heat flow that includes shear heating using 20 MPa stress at all depths. **b**, Heat-flow values projected along the Hikurangi margin, with predicted values. Uncertainties in heat-flow measurements are ± 10 mW m^{-2} (ref. 19).

Because convergence is faster in the north than in the south (Fig. 2a), shear heating on the fault offers a possible mechanism to differentially warm the north and contribute to a shallower transition zone. We tried several values of shear stress but the best agreement with the pattern of heat flow was for $\tau = 20$ MPa (Fig. 3b). Lamb[24] concluded that $\tau \le 10$ MPa for the Hikurangi margin on the basis of balancing plate boundary and topographic forces across the North Island.

Using a uniform 20 MPa of shear stress adds temperatures of 50–100 °C to the fault beneath the forearc (red curves in Fig. 2b) and predicts heat-flow values that agree better with the observed values (Fig. 3). The faster subduction rate in the north results in a higher temperature there relative to the south of about 50–80 °C at 15–40 km depth. To obtain the same temperatures at both the north and south GTZs by shear heating would require over 100 MPa of shear stress, but this would also increase the overall temperatures, pushing heat flow in the forearc well above observed values.

An increase of about 40–50 MPa in shear stress northward along the fault could elevate temperatures in the north by the amount (200–250 °C) needed to put the transition zones in both sections near 350 °C. However, we argue that the stress in the north may be less than in the south. First, the northern Hikurangi subduction zone is outboard of an extensional arc (the Taupo volcanic zone), whereas in the south the upper plate is contracting, indicative of higher stress in the south[24]. Second, the current rate of stress increase on the fault (inferred from geodetic estimates of surface strain rates) in the north seems to be much lower than in the south[10], although this observation itself does not require that the overall stress is lower in the north than in the south.

Although the details of the temperatures derived above for the Hikurangi subduction zone are arguable, it is unlikely that temperature can vary greatly along strike, certainly not enough to maintain the entire GTZ within the 350–450 °C temperature range predicted by some (although the deep transition zone in the south may well be within this temperature range). Clearly, temperature is not the primary controlling factor for the marked along-strike changes in the depths of the GTZ and SSEs. Even by varying the free parameters, it seems that SSEs occur in temperatures about 150 °C lower and depths 20 km shallower in the north than in the south.

Other subduction zones show some evidence for stable sliding at shallow depths. Sagiya[25] describes shallow locking and a SSE along the highly contorted plate interface off the Boso Peninsula in Japan in 1996. Temperatures there are probably much higher than at similar depths off New Zealand because the subducting Philippine Sea plate is much younger than the Pacific (farther south, Oleskevich *et al.*[6] estimate a temperature of 350 °C at 20 km depth). At the Sanak section of the Alaska–Aleutian arc, where the 350 °C isotherm on the fault should be relatively deep[6], free slip starts shallower than at adjacent sections although this depth is poorly constrained[26].

Table 1 Temperature and heat-flow sensitivities.

	Depth (km)	V_t (mm yr^{-1})	V_n (mm yr^{-1})	Age (Myr)	Dip (°)	Stress (MPa)	K_s (W m^{-1} K^{-1})	K_m (W m^{-1} K^{-1})	A_r (µW m^{-3})
ΔP	1.0	5.0	5.0	5.0	1.0	5.0	1.0	1.0	1.0
P_0	15	40	20	80	15	20	2.55	3.30	1.0
ΔT_f	10.9	8.1	−14.0	−3.6	−3.6	16.1	−34.8	1.4	19.1
ΔQ_s	1.8	1.4	−2.4	−0.6	−0.6	2.7	7.8	0.2	3.2
P_0	25	40	20	80	15	20	2.55	3.30	1.0
ΔT_f	10.2	11.5	−23.1	−5.0	−6.0	23.1	−45.1	−7.2	45.5
ΔQ_s	1.0	1.2	−2.4	−0.5	−0.6	2.4	7.8	−0.7	4.6

Most proposed mechanisms for SSEs require them to occur within the frictional stability transition from stick–slip (velocity-weakening) to stable sliding (velocity-strengthening) where small changes to the stress can amplify slip[4,9,27]. If this is true, and the spatial correlation we observe between SSEs and the GTZ is globally robust, then SSEs provide critical information on the nature of the GTZ because it has been interpreted by models ranging from alternating small-scale patches of stick–slip and stable-sliding surfaces[1] to a mathematical convenience to account for mantle relaxation rather than slip on the fault[3]. The close association of the very shallow Hikurangi SSE events with the GTZ clearly identifies the GTZ as a large portion of the fault surface where, intermittently, tens of centimetres of slow fault slip occur. The conditions under which slow slip occurs probably involve material properties of the fault region, fluid interactions, mineralogy and probably other factors not yet recognized. Although the mechanism is still uncertain, we now see that SSEs, even at a single subduction zone, can occur through a wide range of temperature and pressure (depth).

At the northern Hikurangi subduction zone, where only shallow SSEs have been observed so far, geodetic data reveal temporal variations in surface strain rates with periods of the order of decades, possibly related to changes in the depth of subduction coupling through time[28]. Although it has not produced a great thrust earthquake in known history, slip in moderate earthquakes has been emergent and tsunamigenic[29]. Shallow SSEs at depths that are normally seismogenic may modify the rate of strain accumulation and release on multiple timescales and impact each earthquake cycle differently. This likelihood has consequences for earthquake forecasting methods that assume steady strain accumulation between large events.

METHODS

TEMPERATURE ON THE FAULT

We use the derivation by Molnar and England[16] to estimate the temperature T_f at depth z on the Hikurangi thrust fault.

$$T_f(z) = K_m T_0 z / S K_s [\pi\kappa(t_0+t_s)]^{1/2}$$

$$\text{where } S = 1 + bK_m[(V_n z \sin\delta)/\kappa]^{1/2}/K_s.$$

T_0 is mantle temperature (1,300 °C), K_m is mantle thermal conductivity (3.3 W m^{-1} K^{-1}), K_s is the forearc thermal conductivity (2.55 W m^{-1} K^{-1}), κ is the thermal diffusivity (10^{-6} m^2 s^{-1}), t_0 is the age of the incoming lithosphere (80 Myr), t_s is the time it takes the lithosphere to subduct to a depth z, V_n is the convergence rate normal to the subduction zone, δ is the dip angle and b is a factor that depends on the specific geometry[16]. Contours shown in Fig. 2b are derived from a series of profiles spaced at 50 km along the deformation front and we assume horizontal heat flow is negligible. The time t_s is estimated by dividing the integrated downdip length of the fault surface by V_n. The dip angle δ is the average dip between the point at depth z and the deformation front at the surface.

THERMAL CONDUCTIVITY

Well data in the Hikurangi forearc give thermal conductivity values K_s, from south to north, of 2.8 W m^{-1} K^{-1} (Titihaoa-1; 40.7° S), 3.0 W m^{-1} K^{-1} (HawkeBay1; 39.3° S) and 3.6 W m^{-1} K^{-1} (Opoutama-1; 39.1° S)[21]. The northward increase in conductivity coupled with the nearly constant heat flow rule out higher fault temperatures in the north. We adopt the lower value (2.55 W m^{-1} K^{-1}) used by Henrys *et al.*[20]

RADIOGENIC HEAT PRODUCTION

Heat generation in the forearc crust by radiogenic decay results in temperature increases of:

$$T_f(z) = A_r z^2/(2K_s S),$$

where A_r is the radiogenic heat production rate in microwatts per cubic metre. Estimates of heat production in the Hikurangi forearc are lacking, but other subduction zone forearcs show a range of 0.5–1.7 µW m^{-3} (ref. 22). For this range, radiogenic heat production adds less than 4 ± 2 mW m^{-2} to surface heat flow and less than 30 ± 15 °C to the fault temperature below the forearc where the fault is shallower than 20 km.

SHEAR HEATING

Shear heating depends on the shear stress τ on the fault and the total slip rate V_t, and leads to temperature increases of:

$$T_f(z) = \tau V_t z / S K_s.$$

The shear stress τ on a gently dipping fault at shallow depths is approximately $\gamma\,(\sigma_n - p)$, where γ is the coefficient of friction, σ_n is the normal stress on the fault, approximately the overburden pressure, and p is the pore fluid pressure. For $\gamma = 0.85$, $\sigma_n = \rho g z$ (density $\rho = 2{,}500$ kg m^{-3}, gravity $g = 9.8$ m s^{-2}) and $p = 0.95\sigma_n$, the effective shear stress (in megapascals) at any depth is approximately equal to the depth (in kilometres). Hence, the average stress between the surface and 40 km depth on the Hikurangi fault may be about 20 MPa, the value we use. Accordingly, a depth-dependent shear stress would result in lower temperature changes at shallow depths.

HEAT-FLOW PREDICTIONS

If the temperature structure of the forearc is in steady state and there is little heat production within it, the thermal profile from the top of the slab to the sea floor will be approximately linear and we can estimate the vertical temperature gradient by dividing the fault temperature by the fault depth. The heat flow is the thermal conductivity K_s multiplied by this gradient.

SENSITIVITIES OF TEMPERATURE AND HEAT FLOW TO ASSUMED PARAMETERS

Table 1 lists the changes in fault temperature ΔT_f (in degrees Celsius) and in surface heat flow ΔQ_s (in milliwatts per square metre) relative to changes ΔP in the assumed parameters, numerically evaluated at the parameter values P_0 and at depths of 15 and 25 km; $\Delta T_f = T_f(P_0 + \Delta P/2) - T_f(P_0 - \Delta P/2)$ and $\Delta Q_s = Q_s(P_0 + \Delta P/2) - Q_s(P_0 - \Delta P/2)$. In this sensitivity test, V_t and V_n are assumed to be independent and are seen to have opposite influences on T_f and Q_s; an increase in V_n cools the fault owing to advection, whereas increasing V_t warms the fault by shear heating. The influences of increasing K_s are to decrease T_f but increase Q_s. None of these parameters seems to be able to increase the temperature in the northern Hikurangi subduction zone by 250 °C while maintaining nearly uniform heat flow along strike.

Received 20 November 2007; accepted 6 March 2008; published 6 April 2008.

References

1. Scholz, C. *The Mechanics of Earthquakes and Faulting* 2nd edn (Cambridge Univ. Press, Cambridge, 2002).
2. Hyndman, R. D. & Wang, K. Thermal constraints on the zone of major thrust earthquake failure: The Cascadia subduction zone. *J. Geophys. Res.* **98**, 2039–2060 (1993).
3. Wang, K., Wells, R., Mazzotti, S., Hyndman, R. D. & Sagiya, T. A revised dislocation model of interseismic deformation of the Cascadia subduction zone. *J. Geophys. Res.* **108**, 2026 (2003).
4. Liu, Y. & Rice, J. R. Spontaneous and triggered aseismic deformation transients in a subduction fault model. *J. Geophys. Res.* **112**, B09404 (2007).
5. Schwartz, S. Y. & Rokosky, J. M. Slow slip events and seismic tremor at circum-Pacific subduction zones. *Rev. Geophys.* **45** doi:2006RG000208 (2007).
6. Oleskevich, D., Hyndman, R. D. & Wang, K. The updip and downdip limits to great subduction earthquakes: Thermal and structural models of Cascadia, S. W. Japan, Alaska, and Chile. *J. Geophys. Res.* **104**, 14965–14991 (1999).
7. Dragert, H., Wang, K. & James, T. S. A silent slip event on the deeper Cascadia subduction interface. *Science* **292**, 1525–1528 (2001).
8. Linde, A. T., Gladwin, M. T., Johnston, M. J. S. & Gwyther, R. L. A slow earthquake sequence on the San Andreas fault. *Nature* **383**, 65–68 (1996).
9. Lowry, A. P. Resonant slow fault slip in subduction zones forced by climatic load stress. *Nature* **442**, 802–805 (2006).
10. Wallace, L. M., Beavan, J., McCaffrey, R. & Darby, D. Subduction zone coupling and tectonic block rotations in the North Island, New Zealand. *J. Geophys. Res.* **109**, B12406 (2004).
11. Reyners, M. Plate coupling and the hazard of large subduction thrust earthquakes at the Hikurangi subduction zone, New Zealand. *N. Z. J. Geol. Geophys.* **41**, 343–354 (1998).
12. Beavan, J., Wallace, L. M., Fletcher, H. J. & Douglas, A. in *Dynamic Planet: Monitoring and Understanding a Dynamic Planet with Geodetic and Oceanographic Tools, International Association of Geodesy Symposia, 130, Cairns, Australia, 22–26 August, 2005* (eds Tregoning, P. & Rizos, C.) 438–444 (Springer, Berlin, 2007).
13. Douglas, A., Beavan, J., Wallace, L. & Townend, J. Slow slip on the northern Hikurangi subduction interface, New Zealand. *Geophys. Res. Lett.* **32**, L16305 (2005).
14. McCaffrey, R., Wallace, L., Beavan, J. & Douglas, A. Slow slip events, temperature, and interseismic coupling at the Hikurangi subduction zone, New Zealand. *Eos Trans. AGU* **88** (2007). Jt. Assem. Suppl. Abstract G31A-05.
15. Wallace, L. M. & Beavan, J. A large slow slip event on the central Hikurangi subduction interface beneath the Manawatu region, North Island, New Zealand. *Geophys. Res. Lett.* **33**, L11301 (2006).
16. Molnar, P. & England, P. Temperatures in zones of steady-state underthrusting of young oceanic lithosphere. *Earth Planet. Sci. Lett.* **131**, 57–70 (1995).
17. Mortimer, N. & Parkinson, D. Hikurangi Plateau; a Cretaceous large igneous province in the Southwest Pacific Ocean. *J. Geophys. Res.* **101**, 687–696 (1996).
18. Ansell, J. H. & Bannister, S. C. Shallow morphology of the subducted Pacific plate along the Hikurangi margin, New Zealand. *Phys. Earth Planet. Inter.* **93**, 3–20 (1996).
19. Townend, J. Estimates of conductive heat flow through bottom-simulating reflectors on the Hikurangi and southwest Fiordland continental margins, New Zealand. *Mar. Geol.* **141**, 209–220 (1997).
20. Henrys, S. A., Ellis, S. & Uruski, C. Conductive heat flow variations from bottom-simulating reflectors on the Hikurangi margin, New Zealand. *Geophys. Res. Lett.* **30** doi:10.1029/2002GL015772 (2003).
21. Gosnold, W. D. Jr & Panda, B. *Proc. of the Fifth International Mtg, Heat Flow and Structure of the Lithosphere, Kostelec, Czechia* 22 (2001) http://www.geo.lsa.umich.edu/IHFC/heatflow.html.
22. Grevemeyer, I., Diaz-Naveas, J. L., Ranero, C. R., Villinger, H. W. & Ocean Drilling Program Leg 202 Scientific Party. Heat flow over the descending Nazca plate in central Chile, 32° S to 41° S: Observations from ODP Leg 202 and the occurrence of natural gas hydrates. *Earth Planet. Sci. Lett.* **213**, 285–298 (2003).
23. Lewis, K. B., Collot, J.-Y. & Lallemande, S. E. The dammed Hikurangi Trough: A channel-fed trench blocked by subducting seamounts and their wake avalanches (New Zealand-France GeodyNZ Project). *Basin Res.* **10**, 441–468 (1998).
24. Lamb, S. Shear stresses on megathrusts: Implications for mountain building behind subduction zones. *J. Geophys. Res.* **111**, 1–24 (2006).
25. Sagiya, T. Interplate coupling in the Kanto District, Central Japan, and the Boso Peninsula silent earthquake in May 1996. *Pure Appl. Geophys.* **161**, 2327–2342 (2004).
26. Fournier, T. J. & Freymueller, J. T. Transition from locked to creeping subduction in the Shumagin region, Alaska. *Geophys. Res. Lett.* **34** doi:10.1029/2006GL029073 (2007).
27. Rubinstein, J. L. *et al*. Non-volcanic tremor driven by large transient shear stresses. *Nature* **448**, 579–582 (2007).
28. Arnadottir, T. S., Thornley, S., Pollitz, F. & Darby, D. Spatial and temporal strain rate variations at the northern Hikurangi margin, New Zealand. *J. Geophys. Res.* **104**, 4931–4944 (1999).
29. Doser, D. I. & Webb, T. H. Source parameters of large historical (1917–1961) earthquakes, North Island, New Zealand. *Geophys. J. Int.* **152**, 795–832 (2003).
30. Beavan, J., Tregoning, P., Bevis, M., Kato, T. & Meertens, C. Motion and rigidity of the Pacific plate and implications for plate boundary deformation. *J. Geophys. Res.* **107**, 2261 (2002).

Acknowledgements

R. Sutherland, M. Reyners and Y. Liu provided helpful comments on the manuscript. Funding for this work was provided by the New Zealand Earthquake Commission (EQC), the New Zealand Foundation for Research, Science and Technology and GNS Science.

Author information

Reprints and permission information is available online at http://npg.nature.com/reprintsandpermissions. Correspondence and requests for materials should be addressed to R.M.